JOURNAL OF Applied Polymer SCIENCE

Microstructural Characterization of Corn Starch-Based Porous Thermoplastic Composites Filled with Multiwalled Carbon Nanotubes

Hilmi Yurdakul,[1] Oya Durukan,[1] A. Tugrul Seyhan,[1] Hande Celebi,[2] Mustafa Oksuzoglu,[1] Servet Turan[1]

[1]Department of Materials Science and Engineering, Anadolu University, Iki Eylul Campus, 26550 Eskisehir, Turkey
[2]Department of Chemical Engineering, Anadolu University, Iki Eylul Campus, 26550 Eskisehir, Turkey

Correspondence to: A. T. Seyhan (E-mail: atseyhan@anadolu.edu.tr)

ABSTRACT: Microstructural characterization of corn starch-based porous thermoplastic (TPS) composites containing various contents (0.1, 0.5, and 1 wt %) of multiwalled carbon nanotubes (MWCNTs) was performed. Corn starch was plasticized with a proper combination of glycerol and stearic acid. TPS composites with MWCNT were prepared conducting melt extrusion followed by injection molding. TPS containing 1 wt % of MWCNTs exhibited higher tensile strength and elastic modulus values than neat TPS. Moreover, TPS electrical conductivity was determined to increase with increasing content of MWCNTs. X-ray diffraction measurements revealed that incorporation of MWCNTs increased the degree of TPS crsystallinity to some extent. Scanning electron microscopy examination revealed that MWCNT altered TPS surface morphology and tensile failure modes, significantly. Transmission electron microscopy investigation showed that dispersion characteristics of MWCNTs within TPS were in the form of tiny clusters around micro pores of TPS, which is considered influential on electrical conductivity of the resulting composites. © 2012 Wiley Periodicals, Inc. J. Appl. Polym. Sci. 000: 000–000, 2012

KEYWORDS: Multiwalled carbon nanotubes (MWCNTs); extrusion; injection molding

Received 10 January 2012; accepted 27 March 2012; published online
DOI: 10.1002/app.37794

INTRODUCTION

Synthetic polymers derived from petroleum, a limited, nonrenewable resource, have been produced commercially on a very large scale and their use in disposable items has grown significantly.[1–6] Nevertheless, the large proportion of the synthetic polymers has been a matter of concern because most of the synthetic polymers do not degrade completely and cause serious environmental problems.[4–15] Renewable source-based polymers have recently emerged as an eco-friendly alternative to synthetic polymers. Starch has been cited as one of the most promising renewable source based polymers because of its large scale of availability combined with low cost.[1–4] Starch is a natural renewable polysaccharide and exists in the form of fine white granules composed of amylose and amylopectin accompanied by the basic composite unit of glucose. Preparation of starch-based polymer (SBP) involves various complicated chemical and physical reactions including water diffusion, gelatinization, decomposition, melting, and crystallization.[2,11] Among these reactions, gelatinization is by far the most essential, as it constitutes the starting point for conversion of starch into thermoplastic material. Moreover, SBP can not be thermally processed without using a plasticizer, as its decomposition temperature is much lower than its melting temperature prior to gelatinization.[5] With the aid of plasticizer, the starch becomes suitable for processing through mechanical shear at elevated temperature and then turns into an essentially homogenous material. To accomplish commercially acceptable products, starch is usually blended with other polymeric materials to improve its physical properties and to minimize or eliminate water sensitivity.[7,10,14] However, in this case, proper adjustment of processing temperature and dwell time is certainly required to compensate for the rheological property differences between SBP and the polymeric material of interest. On the other hand, blending low content of nanofiller constituents such as nanoclay or carbon nanotube (CNT) with SBP is a relatively feasible way towards improving the SBP properties as well.[2,6] CNT with huge aspect of ratio and surface area combined with outstanding mechanical and electrical properties is commonly employed to manufacture electrically conductive polymer composites with enhanced mechanical properties.[2–5] However, CNT tends to agglomerate because of

its huge surface area. Therefore, accomplishment of homogeneous dispersion of CNTs within polymers is essential in terms of polymer property enhancements.[16–19] In the case of blending SBP with CNT, the utmost attention is to be paid to homogenous dispersion of CNTs within SBP throughout blending.

Various techniques including melt extrusion, injection molding, and film casting, successfully used for processing of synthetic polymers, can also be conducted for processing of SBP. Nevertheless, the inevitability of proper gelatinization makes it difficult to control processing of SBP as compared to processing of synthetic polymers.[7,10] In the absence of shear stress, gelatinization depends essentially on water content and temperature conditions.[11] However, water content is critical to proper gelatinization of starch under shearless conditions. If there is excess water, the starch crystallites may be pulled apart by swelling, leaving nothing to melt at high temperatures. If there is a little water, the swelling forces become insignificant and proper gelatinization does not occur in the low temperature range. Shear stress makes possible the separation of amylose from amylopectin to some extent. It is for this reason that melt extrusion with uniform temperature distribution under mechanical shear is the best way possible to yield more amorphous starch. However, SBP, when allowed to come to the equilibrium, retrograde and recrystallize into various crystal polymorphs, depending on relative humidity, the type and content of the plasticizers, fillers, and temperature conditions.[5] It is worthy of attention that CNTs with huge aspect ratio and surface area, when mixed with SBP under shear, may affect the characteristics properties of the resulting structure.

There are a few studies in the literature, which focused on preparation and characterization of SBP/CNT composites. Xiadong et al.[3] utilized acid treated multiwalled carbon nanotubes (MWCNT) as reinforcing constituent to enhance the ultimate performance of glycerol plasticized pea starch. They prepared the composite films, using solution casting followed by evaporation. They found that composite films containing 3 wt % of MWCNTs exhibited, respectively, 50 and 90% higher tensile strength and elastic modulus values than neat composite films. In another study, Ma et al.[14] prepared glycerol plasticized-corn starch composites with MWCNTs, using solution casting. They concluded that the presence of MWCNTs precluded starch recrystallization and improved the tensile strength and modulus of the SBP while reducing its toughness. They also revealed that the composite films showed a water dependent electrical conductivity up to a critical content of MWCNTs (3.8 wt %). Fama et al.[17] treated the MWCNT surfaces with an aqua solution of starch-iodine complex and then blended the treated MWCNT with the same matrix of starch. They finally reported that composites with treated MWCNT showed 35% higher tensile strength than neat SBP. Similar study was also performed by Zhanjun et al.[18] utilized carboxylated MWCNT as nanofillers to improve the performance of SBP. They found that addition of treated MWCNT below 1.5 wt % led to a remarkable increase in the SBP thermal stability.

In this study, a lab-scale extruder was conducted to blend different contents of MWCNTs with a native corn starch, using glycerol and stearic acid as plasticizers. The ribbons obtained at the end of extrusion was cut into smaller pieces and then injection-molded into dog bone shapes for tensile mechanical property characterization. X-ray diffraction (XRD) was used to gain some insight into MWCNT induced effects on TPS crystalline structure. Electrical conductivity of the produced samples was also measured. Scanning electron microscopy (SEM) and transmission electron microscopy (TEM) were employed to examine the fracture surface morphology and to visualize the dispersion state of MWCNTs within TPS, respectively. Combining TEM images and electrical conductivity values, it was determined that electrical conductivity and tensile mechanical properties are highly dependent on the preferential CNT distribution around TPS micropores. Please note that to our best knowledge, melt extrusion and injection molding were for the first time used in the literature in order to prepare MWCNT modified SBP samples of representative sizes. Finally, an assessment of the results was made with an emphasis on discussing the interactions among corn starch, the plasticizers, and MWCNTs.

EXPERIMENTAL

Materials

Native corn starch composed of 30% wt of amylose and 70% wt of amylopectin was provided by Bizim Limited in Turkey. Industrial grade glycerol (98% purity) and stearic acid in the powder form were obtained from Sigma-Aldrich and Fisher Scientific, respectively. They were both used as plasticizers. High conductive grade of MWCNTs produced by chemical vapor deposition were obtained from Nanocyl, Namur Belgium. MWCNT with a length of several micrometers up to 50 μm has average outer and inner diameters of 3.2 and 2.8 nm, respectively.

Preparation of MWCNT Mofidied Thermoplastic Starch

Stearic acid was dissolved in a mixture of glycerol and water (1: 10 w/w), using a magnetic stirrer at 40°C for 30 min. Simultaneously, various contents (0.1, 0.5, and 1 wt %) of MWCNTs accompanied by a certain amount of corn starch were dispersed within vinegar containing 5 wt % of acetic acid, using a high shear mechanical stirrer for 30 min. Note that use of vinegar helps break up amylopectin branches of starch, with the resulting SBP not being highly brittle. The dissolved stearic acid solution was then put in the prepared vinegar dispersion and the resulting suspension was subjected to sonication (Sonics Vibration 750 W) for 30 min to make sure the proper dispersion of all the ingredients in the suspension. Note that the resulting suspension was composed of 5 wt % of corn starch, 6.5 wt % of glycerol, 1 wt % of stearic acid, 61.5 wt % of deionized water, and 26 wt % of vinegar. By means of a magnetic stirrer, the suspensions with and without MWCNT were subjected to preheating at 75°C until their viscosity was high enough for melt extrusion. The preheated suspensions were then manually fed into the extruder. The complete plasticization (full gelatinization) of the preheated stuff was achieved in a DSM Xplore twin-screw mini extruder with a volume of 15 mL. The temperatures of the feed, metering, compression, and die sections in the extruder barrel were set at 110, 140, 140, and 140°C, respectively. The screw speed was kept at 25 rpm for the first 5 min

and then increased up to 75 rpm for the rest of the process. Note that the mechanical torque value generated in the extrusion barrel was taken into account to set the dwell time for proper gelatinization throughout extrusion. The extruded TPS ribbons was cut into separate long strands and used as raw materials for injection molding. DSM Xplore micro injection molding machine with a volume of 12 mL was used to prepare the tensile testing coupons. Figure 1(a,b) shows the cut separate long strands and the injection molded dog bone shaped tensile coupons, respectively. During injection molding, temperatures of the injection, post injection and cooling sections of the machine were all set at 110°C, while the screw speed and the injection pressure were adjusted to 0.02 m/s and 6 bars, respectively. The produced dog-bone tensile test coupons were allowed to equilibrate at room temperature (40–50% relative humidity) for three weeks prior to their property characterizations.

XRD Examination

The crystalline structures of corn starch powder, neat MWCNT, neat TPS, and TPS composites containing 0.1, 0.5, and 1 wt % of MWCNTs were examined via XRD measurements. Corn starch powder and neat MWCNT were used as received, while TPS and its composites were compressed into thin flat sheets with a thickness of 1 mm before placed into a sample holder. XRD patterns were collected using a Bruker AXS D8 4-circle diffractometer equipped with a Cu sealed tube point source. A Göbel Mirror optic generating a 2D-collimated parallel beam (divergence ca. 0.03° and a lateral length of 18 mm) was used to collect the data. Monochromatic Cu–Kα radiation (wavelength =1.5405 Å) and an antiscatter slit were conducted to remove background resulting from square samples of 10 × 10 mm^2. X-ray beam was generated at 40 kV to 30 mA. The scanning regions of the diffraction angle (2Θ) varied from 3° to 40°, which covered all the significant diffraction peaks of the starch crystallites. Note that XRD measurements aimed to gain some insights into the MWCNT induced effects on the TPS crystal structures. X-ray diffractograms of the TPS and its composites were correlated with a baseline, using Bruker Topas-3 software. The degree of crsystallinity for all samples was computed based on the procedure prepared by Wang et al.[15]

Mechanical Property Characterization

Tensile mechanical properties of the neat TPS and its composites with different content of MWCNT were determined at room temperature according to DIN EN ISO 527.1, using an Instron 5541 testing machine equipped with a 2 kN loading cell. Tests were carried out at a crosshead speed of 5 mm/min on the samples with a gauge length of 20 mm. An average of five replicates for each sample was taken into account during data interpretation.

Microscopic Characterization

To reveal MWCNT induced effects on TPS failure modes and morphology, fracture surfaces of the samples were examined, conducting a Schottky emitter field emission gun (FEG)-SEM (SEM-Zeiss SUPRA 50 VP) attached with In-Lens and Back scattered (BS) detectors in variable pressure (VP) mode at an acceleration voltage of 1 kV. Furthermore, TEM was used to visualize the dispersion state of MWCNTs within TPS. TEM sample films with a thickness of 70 nm were prepared at −60°C by using a cryogenic ultra-microtome. TEM studies were performed by conducting FEG-TEM (TEM-Jeol 2100F) coupled with a scanning transmission electron microscopy-high angle annular dark field (STEM-HAADF) detector. High resolution transmission electron microscopy (HR-TEM) was also conducted to visualize the interfacial interactions between MWCNTs and the plasticizers.

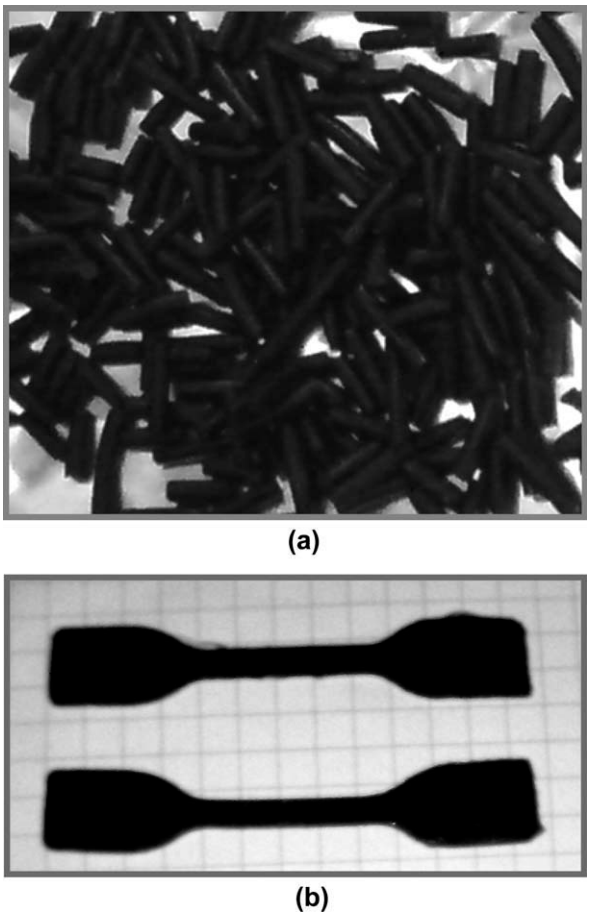

Figure 1. Photo of (a) the extruded separate long strands and (b) the injection molded dog bone shaped tensile coupons.

Electrical Property Characterization

All the samples with and without MWCNT were compressed into thin flat sheets prior to electrical property characterization. Electrical resistance and resistivity measurements with a voltage of 1.0 V were subsequently carried out on the square samples (10 × 10 mm^2) with a thickness of 2 mm, using a Lucas Labs Pro-4 Four Point Probe. The value of electrical conductivity for each sample was then calculated from the electrical resistivity values.

RESULTS AND DISCUSSION

XRD Measurements

Figure 2(a) gives the XRD patterns for the corn starch granules and pristine MWCNT. Pristine MWCNT shows only one peak, making a sharp (002) Bragg reflection at about 2θ values of

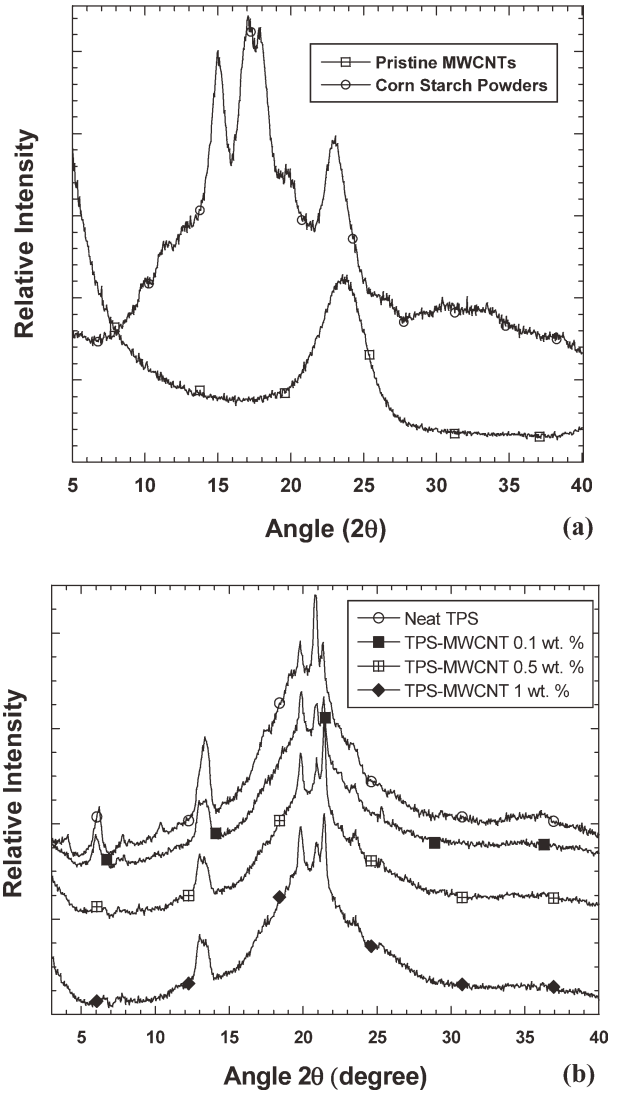

Figure 2. (a) XRD patterns of corn starch granules and pristine MWCNT, (b) XRD patterns of TPS and its composites with different contents of MWCNTs.

23.4° because of the ordered array of the concentric graphitic cylinders.[16,17] On the other hand, within corn starch powder, relatively high crystalline peaks are significantly noticeable. In particular, the starch powder gives the peaks at 2θ values of 15.30°, 19.87°, and 22.98°.[2,11,15] This result revealed that the starch contains B-crystal type of structures. On the other hand, one major peak splits into two separate peaks at 2θ values of 17.1° and 17.93°, which both correspond to the A crystal type of structures. In the light of these findings, it was concluded that the starch powder is mainly composed of A and B type crystal structures. Figure 2(b) gives the XRD patterns for neat TPS and its composites with different content of MWCNTs. Regardless of MWCNT content, TPS was found to retain almost all of its characteristic crystalline peaks. Note that, on the basis of the nanofiller peak intensity values, XRD can be effectively used to gain an insight into dispersion state of the corresponding nanofillers within polymers. Regardless of MWCNT content, TPS composites were found not to exhibit any remarkable sign of peak apparent at 2θ values of 23.4°, which corresponds to (002) Bragg reflection of MWCNTs. This indicated that proper dispersion of MWCNTs within TPS that was successfully accomplished. Please note that it is a big challenge to disperse the pristine MWCNT separately within TPS during melt extrusion due to huge surface energy difference between pristine MWCNT and TPS matrix.[11,16–19] In other words, since the as-received MWNCTs are hydrophobic, it can be expected the MWCNTs to be agglomerated in the corn starch-based polymer, which is hydrophilic. Please bear in mind that the nonexistence of the characteristic peak of CNT at around 2θ values of 23.4° in XRD patterns may be resulting from very low content of CNTs within TPS matrix. In this case, this peak may have overlapped with the peak at around 2θ values of 22.98°, which belongs to TPS structure. In other words, this means that the results obtained do not necessarily imply that CNTs were dispersed within TPS individually and homogenously. In addition to this, a small peak at around 2θ values of 23° and 24° is characteristics of TPS with CNTs only and does not appear in the pattern of neat TPS essentially. This peak might indicate a small shift of CNTs within TPS from its original position relative to peak pattern of pristine CNTs, most probably due to shear applied during melt extrusion. Therefore, we search for further ample evidences to shed light on dispersion state of CNTs within TPS. When combined with morphological investigation performed by SEM and TEM, XRD findings are proportional to our approach that CNTs exhibit a preferential distribution around pores within TPS, depending on weight content, which makes it virtually impossible to predict how the resulting composites behave in terms of mechanical or electrical properties.

The intensity of the peaks at 2θ = 5.7° and 2θ = 13.4°, which correspond to B type polymorphs, was found to decrease with increasing content of MWCNTs. Moreover, the intensity of the peaks at 2θ = 19.7° and 2θ = 21.5°, which could be, assigned to B and V type polymorphs, respectively, were revealed to increase with increasing content of MWCNTs. Note that V type polymorphs form directly after melt extrusion, which leads to higher elastic modulus and yield stress for amylose-rich starch.[2] Furthermore, the crystalline peak apparent at 2θ = 20.3° was ascribed to V_h crystallinity that occurs due to interaction between amylose and lipid complexes. Once preheated starch was entirely plasticized during melt extrusion, the amylose, native lipids, and stearic acid were likely to form various helical inclusion complexes that further crystallized into V patterns.[2,11] From this point of view, it could be reasonable to expect MWCNT to improve the degree of crystallinity and toughness of TPS. Based upon the areas under the XRD peaks, neat TPS and its composites containing 0.1, 0.5, and 1 wt % of MWCNTs were found to exhibit 40, 42, 47, and 48% of degree of crystallinity, respectively, which backs up our approach. Moreover, a new tiny peak formed at 2θ = 25.4° within the TPS crystalline structure with MWCNT. Lepifre et al.[20] reported that an extra peak formed at 2θ = 21.5° with the addition of the whiskers to a TPS. They attributed it to the plasticizer accumulation at the interface between starch and whiskers. In our case, the formation of extra peak may, in a similar manner, imply that glycerol

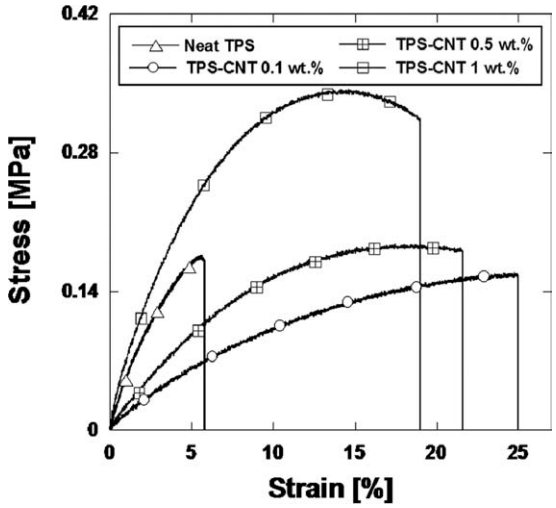

Figure 3. Typical stress–strain behavior of neat TPS and its composites with respect to CNT content.

penetrates into the interface between the MWCNT and the corn starch molecules. This sounds realistic because stearic acid with limited OH groups is bulkier than glycerol and hence is not able to penetrate into or interact with starch polymeric chains as easily as glycerol. In the most likely scenario, glycerol is preferentially located in relatively high crystalline regions of the TPS with MWCNT, whereas stearic acid remains intact within relatively high amorphous regions of TPS with MWCNT. In this scenario, stearic acid, as a processing aid, comes into play later and improves the rheological behavior of TPS during melt extrusion. This occurrence was also confirmed with SEM images taken from TPS fracture surfaces with MWCNTs, as discussed later on in the text.

Tensile Mechanical Properties

Figure 3 gives the typical tensile stress and strain behavior for neat TPS and its composites with different CNT contents. As seen in the figure, regardless of weight content, addition of MWCNTs was found to give rise to TPS toughness values calculated integrating the area under the stress and strain curves. Table I summarizes the corresponding tensile properties for TPS and its composites. As seen in the table, addition of 1 wt % of MWCNTs increased the TPS tensile strength by 55%, while tensile strength values of neat TPS and its composites with 0.1 and 0.5 wt % of MWCNTs scattered more or less around the same value (0.14 MPa). Note that the composites filled with 0.1 and 0.5 wt % of MWCNTs show relatively low elastic modulus and high elongation values than the neat TPS. It is very well known that the degree of polymer crystallinity may be significantly influential on the polymer mechanical properties, since it affects the extent of the intermolecular secondary bonding. For crystalline regions wherein molecular chains are packed in an ordered arrangement, wide-ranging secondary bonding occurs between adjacent chain segments. These bonds lead to especially polymer tensile modulus to increase significantly with degree of crystallinity. However, our results do not comply with the aforementioned general statement. Previously, XRD findings revealed that TPS crystallinity increases with MWCNTs. However, tensile modulus values of TPS were not proportionally improved by the addition of MWCNTs, except for 1 wt % loading rate. This may be due to the presence of acetic acid in vinegar that may result in formation of starch acetates during melt extrusion, which are widely used in biodegradable packaging foams.[2,11] In this scenario, MWCNT content and distribution characteristics play a pivotal role in the way starch acetates chemically form. In other words, this anomalous behavior may be resulting from preferential or virtually unpredictable distribution characteristics of MWCNTs around the micro-pores within TPS structure with respect to weight content. Recalling XRD findings, we should also take into account the TPS crystallization behavior as well. In polymers, surfaces are known to act as catalysts for the nucleation of crystals. In polymers patterned with pores, as in our case, it is possible that the shape of the pores sizes of which show dependency on CNT weight content can control the kinetics of surface-induced crystal nucleation. We can infer from these expressions that kinetics of crystal nucleation are linked to the way starch acetates occur as a function of CNT weight content, which stimulates CNTs to coalesce around the micro-pores formed. To put answers to these questions, SEM and TEM techniques were further conducted.

Figure 4 (a,b) give the SEM images showing the tensile fracture surfaces of neat TPS and its composites with 1 wt % of MWCNTs, respectively. It is obvious that incorporation of MWCNTs altered TPS fracture surface morphology and failure modes significantly. At 1 wt % loading rate, TPS with CNTs were fractured in a ductile manner although their fracture surfaces look like they are fractured in a brittle manner fracture, whereas neat TPS were fractured in a brittle manner making not a remarkable necking before failed. This is most probably due to modified chemistry of TPS in the presence of MWCNTs at different weight content within TPS. These behaviors are highly proportional to the trend observed in the stress–strain behavior of TPS with and without CNTs as depicted in Figure 3. Figure 5(a) is the high magnification SEM image showing the fracture surface of TPS composites containing 1 wt % of MWCNTs, while Figure 5(b) depicts the SEM image of an intentionally selected region, highlighted with a dashed circle in Figure 5(a), at relatively high magnification. As seen in the figures, porous structure is of characteristics of TPS with MWCNTs. Note that the TPS synthesized in this study possessed porous structure as a result of complex chemical reactions that occur mainly between stearic acid, acetic acid, and glycerol. The evaporation of water contained in starch based

Table I. Tensile Properties of TPS with and without MWCNTs

Weight content (wt %)	Elastic modulus (MPa)	Tensile strength (MPa)	Strain at rupture (%)
0	3.39 ± 0.44	0.16 ± 0.03	7 ± 4
0.1	3.14 ± 0.78	0.14 ± 0.02	24 ± 8
0.5	3.21 ± 0.62	0.15 ± 0.04	22 ± 6
1	3.94 ± 0.81	0.29 ± 0.08	18 ± 5

Applied Polymer SCIENCE

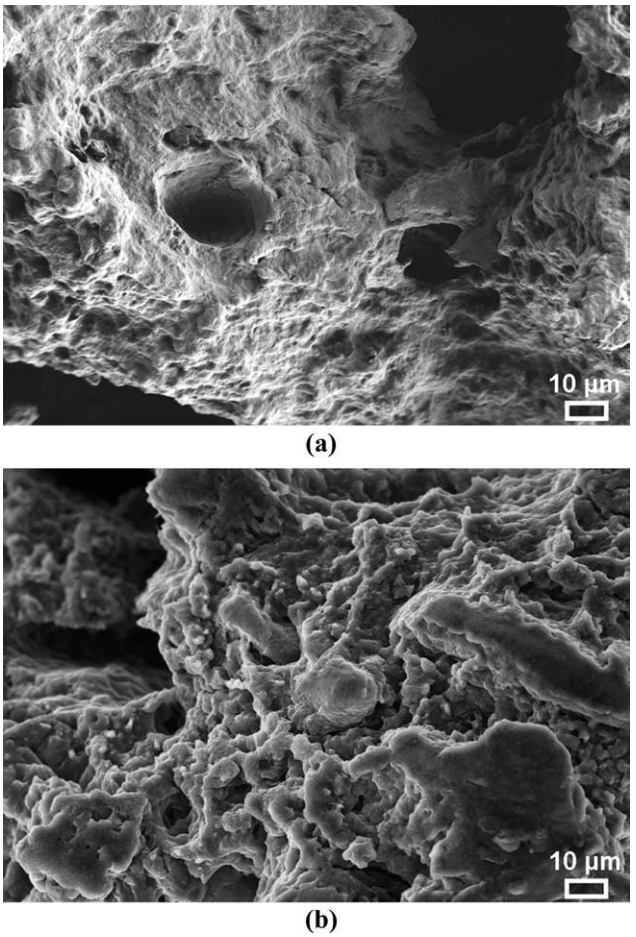

Figure 4. SEM images (a) the neat TPS tensile fracture surfaces (b) TPS composites with 1 wt % of MWCNTs.

materials can also result in undesired bubble formation, which triggers the occurrence of both favorable and unfavorable chemical reactions in the presence of MWCNTs during melt extrusion. More than one of these can be cited as the reason for the TPS to exhibit anomalously low tensile strength and modulus values relative to their equivalences in the literature. Moreover, big white spots in Figure 4(a) refer to undissolved stearic acid particles. More interestingly, in the same figure, MWCNT seem to be accumulating between an individual semigelatinized starch granule and stearic acid particle, which is proportional to the XRD findings. From this point of view, interactions between plasticizers and MWCNTs as well as MWCNT contents are crucial to final TPS properties. In other words, TPS porous structure may, in this case, be highly related to MWCNT content, as stated earlier as our approach. To proceed with this approach, TEM characterization was necessarily needed.

TEM equipped with a HAADF detector was employed to visualize the dispersion state of MWCNTs within TPS matrix. Figure 6(a,b) depict the acquired atomic number (Z)-contrast images of MWCNT modified TPS matrix at different magnifications in STEM-HAADF mode. Note that conventional TEM dark field (DF) images are obtained from the signal emitted by elastic scattering of electrons, whereas STEM-HAADF images come out off the signal emitted by incoherent scattering of electrons at relatively high angles.[21,22] This makes STEM-HAADF capable of offering one to differentiate between the regions of different atomic numbers (Z).[21–24] In Figure 6(a,b), dark regions refer to open pores, while gray regions and white spots, highlighted by arrowheads, refer to TPS characteristics structure and tiny MWCNT clusters, respectively. Moreover, it is worthy of mention that each corresponding region shows distinctly different contrast level, despite their similarity in that their own chemical structures are mainly composed of carbon. Properly speaking, in STEM-HAADF mode, the brighter a phase appears under the microscope, the more crystalline this phase is under the specified diffraction condition.[23] MWCNT consists of multiple stacked single-walled carbon nanotubes with diameters ranging from 2 to 100 nm shows only one peak in the XRD diagram, as given in Figure 2(a,b). This is due to the arrays of well ordered individual concentric cylinders of MWCNTs that make MWCNT behave like a highly crystalline material. In Figure 6(a,b), the difference between the contrast levels of MWCNTs and TPS matrix are certainly noticeable. TPS matrix with a gray contrast color was considered as a semicrystalline material,

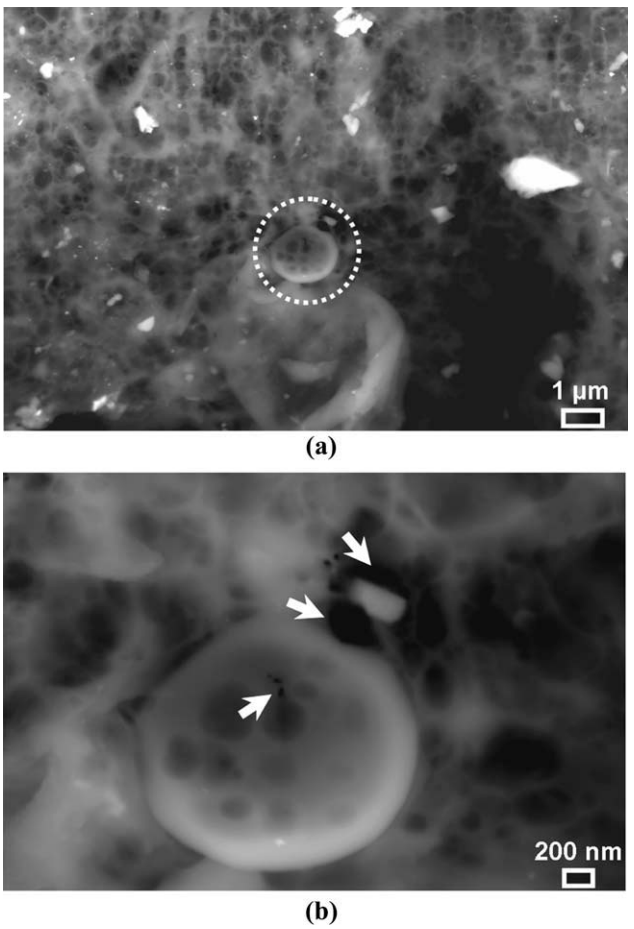

Figure 5. (a) Fracture surface SEM image of TPS composites with 1 wt % of MWCNTs (b) SEM image of a specific region highlighted with a dashed circle in Figure 6(a) at relatively high magnification.

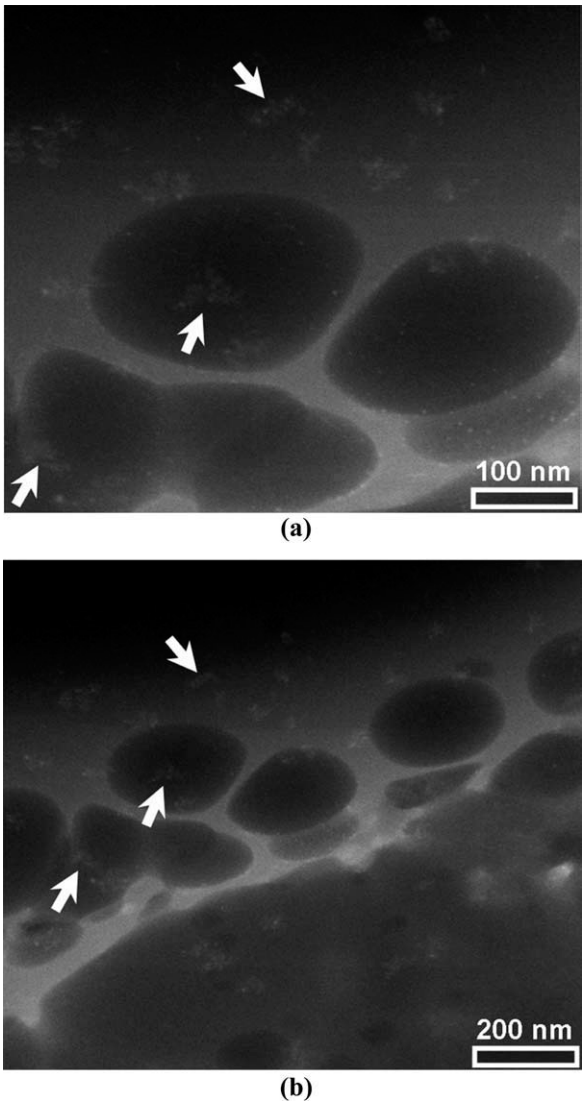

Figure 6. (a, b) *Z*-contrast images of MWCNT modified TPS matrix at different magnifications in STEM-HAADF mode.

which was already confirmed by the XRD findings given in Figure 2(b). In addition, it is highly remarkable that tiny MWCNT clusters are in the majority around the TPS porous structure. Herein the first question that comes to mind is whether the porous structures within TPS matrix result from the highly complicated chemical reactions taking place during complete starch gelatinization or whether they are induced by irradiation during electron beam exposure? For the sake of clarity, the intentionally selected region highlighted in Figure 6(a) was subjected to a continued electron beam exposure at specified time intervals. As a result, it was determined that no remarkable structural change occurred within this region as a function of time, indicating that the porous structures within TPS took place, most likely, because of chemical reactions during starch plasticization. Figure 7(a,b) show HR-TEM images taken from TPS with 1 wt % of MWCNTs at different magnifications. Individual MWCNTs in Figure 7(a) is noticeably visible. Figure 7(b) taken at relatively high magnification, from the white lined circular region apparent on the left side of Figure 7(a) depicts the interaction at the interface among MWCNTs, the plasticizers used and TPS matrix. The contrast level at the interface backs up our approach that MWCNTs accumulate between the plasticizers and the starch matrix. These findings are vastly proportional to those obtained from SEM images [Figure 5(a,b)]. Figure 8 shows the electrical conductivity of neat TPS and its composites containing different content of MWCNTs. It was determined that electrical conductivity of composites increased with increasing content of MWCNTs. In particular, TPS with 1 wt % of MWCNTs exhibited two orders of magnitude higher electrical conductivity value than neat TPS. In contrast to mechanical property enhancement of polymers via CNT, where a tailored interface with the strong adhesion of individual CNT to the surrounding polymer matrix is prerequisite, the electrical conductivity enhancement for polymers is just dependent on percolated pathways of tiny CNT clusters. In other words, small agglomerates accompanied by individual CNTs are highly preferable in terms of polymer electrical conductivity enhancement.

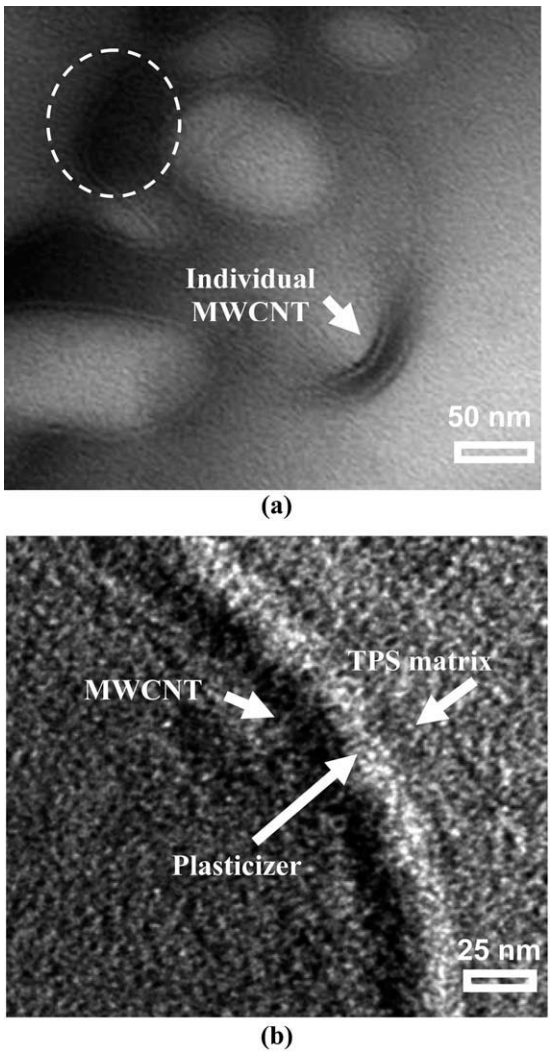

Figure 7. (a, b) HR-TEM images showing the interaction at the interface between MWCNTs and the plasticizers at 1 wt % loading rate of MWCNTs.

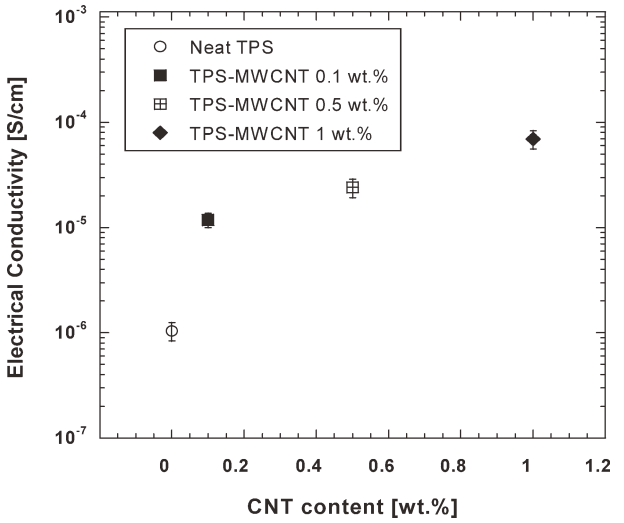

Figure 8. Electrical conductivity values of TPS with respect to MWCNT weight contents.

Therefore, the quantity and distribution of tiny CNT clusters within a polymer matrix is critical to enhancing the electrical conductivity of a polymer matrix. SEM and STEM images showed that the dispersion characteristic of MWCNTs within TPS was in the form of tiny clusters, which is highly favorable to electrical conductivity enhancement. On the other hand, neat TPS exhibited, unexpectedly, as high electrical conductivity as a common synthetic thermoplastic polymer with a low content of conductive filler. Since starch is hydrophilic, water absorption capability of starch is important to performance of starch based biodegradable polymers. Ma et al.[14] showed that the conductivity of the TPS was improved by five orders of magnitude once water content was increased by a factor of six. More importantly, they found that the higher content of MWCNTs within TPS, the less water-dependency TPS electrical conductivity shows. Moreover, since the TPS synthesized in this study possess semiporous structure, they could absorb more water than their bulk counterparts within the same intended time for equilibrium (three weeks prior to property characterization). As a result, due to their high water absorption capability, neat TPS showed almost as high electrical conductivity as TPS with MWCNTs.

CONCLUSIONS

This study focuses on the preparation and characterization of TPS composites with various contents of MWCNTs. TPS composites were produced via melt extrusion followed by injection molding. Glycerol and stearic acid were used as plasticizers to gelatinize the corn starch. XRD measurements showed that incorporation of MWCNTs at 1 wt % loading rate increased the degree of TPS crystallinity by 20%. Moreover, TPS composites with 1 wt % of MWCNTs exhibited considerably higher tensile strength and elastic modulus than neat TPS. However, incorporation of MWCNTs did not mirror the same profound effect at relatively low loading rates (0.1 and 0.5 wt %) on TPS tensile mechanical properties, although highly beneficial to TPS toughness enhancement regardless of weight content. In addition, it was also determined that TPS composites with MWCNT exhibited almost two orders of magnitude higher electrical conductivity value than neat TPS. SEM examination revealed that TPS fracture surface morphology was profoundly affected by the presence of MWCNTs. STEM investigation showed that tiny MWCNT clusters are preferentially located around the TPS pores, which contributed to TPS electrical conductivity. HR-TEM images backed up our approach that MWCNTs accumulate among the plasticizers, specifically between stearic acid and the thermoplastic starch matrix. The future study will unveil the MWCNT induced effects on the crystallization kinetics of neat TPS.

ACKNOWLEDGMENTS

The authors would like to acknowledge NANOCYL, Namur in Belgium for encouraging this study by providing us with high conductive grade MWCNT free of charge.

REFERENCES

1. Chin-San, W.; Hsin-Tzu, L. *Polymer.* **2007,** *48*, 4449.
2. Hongsheng, L.; Fengwei, X.; Long, Y.; Ling, C.; Lin, L. *Prog. Polym. Sci.* **2009,** *34*, 1348.
3. Xiadong, C.; Yun, C.; Peter, C. R.; Huneault, A. M. *Polym. Sci.* **2007,** *106*, 1431.
4. Xiaofei, M.; Peter, C. R.; Jiugao, Y.; Peilin, L. *Carbohydr. Polym.* **2008,** *74*, 895.
5. Natta, L.; Athapol, N. *Starch* **2004,** *56*, 348.
6. Yi-Lin, C.; Seema, A.; Luis, E.; Suren, H.; Emmanuel, G. P.; Hsi-Mei, L. *Carbohydr. Polym.* **2010,** *79*, 391.
7. Wang, S.; Yu, J. *Polym. Degrad. Stab.* **2005,** *87*, 395.
8. Jin-hui, Y.; Jiu-gao, Y.; Xiao-fei, M. *Starch* **2006,** *58*, 580.
9. Jin-Hui, Y.; Jiu-gao, Y.; Xiao-fei, M. *Carbohydr. Polym.* **2006,** *63*, 218.
10. Cañigueral, N; Vilaseca, F; Méndez, J. A.; López, J.;, Barberà, L.; Puig, J; M. A. Pèlach, Mutjé, P. *Chem Eng Sci* **2009,** *64*, 2651.
11. Halley, P. J.; Truss, R. W.; Markotsis, M. G.; Chaleat, C.; Russo, M.; Sargent, A. L.; Tan, I.; Sopade, P. A. In Polymer Durability and Radiation Effects; Celina, M. C., Assink, R. A., Eds; American Chemical Society: United States, **2007;** p 287–300.
12. Ming-Fu, H.; Jiu-Gao, Y.; Xiao-Fei, M. *Polymer* **2004,** *45*, 7017.
13. Garcia-Gutierrez, M. C.; Nogales, A.; Hernandez, J. J.; Rueda, D. R.; Ezquerra, T. A. *Opt. Pura Apl* **2007,** *40*, 195.
14. Ma, X. F.; Yu, J. G.; Wang, N. *Carbohydr. Polym.* **2007,** *67*, 32.
15. Wang, S.; Yu, J.; Gao, W. *Am. J. Biochem. Biotech.* **2005,** *4*, 207.
16. Xiaofei, M.; Jiugo, Y.; Ning, W. *Comp. Sci. Tech.* **2008,** *68*, 268.

17. Fama, L. M.; Pettarin, V.; Goyanes, S. N.; Bernal, C. R. *Carbohydr. Polym.* **2011,** *83*, 1226.
18. Zhanjun, L.; Lei, Z.; Minnan, C.; Jiugao, Y. *Carbohydr. Polym.* **2011,** *83*, 447.
19. Yurdakul, H.; Seyhan, A. T.; Turan, S.; Tanoglu, M.; Bauhofer, W.; Schulte, K. *Comp. Sci. Tech.* **2010,** *70*, 2102.
20. Lepifre, S.; Froment, M.; Cazaux, F.; Houot, S.; Lourdin, D.; Coqueret, X.; Lapierre, C.; Baumberger, S. *Biomacromolecules* **2004,** *5*, 1678.
21. Pennycook, S. J. *Annu. Rev. Mater. Sci.* **1992,** *22*, 171.
22. Varela, M.; Lupini, A. R.; Benthem, K. V.; Borisevich, A. Y.; Chisholm, M. F.; Shibata, N.; et al. *Annu. Rev. Mater. Res.* **2005,** *35*, 539.
23. Pennycook, S. J.; Lupini, A. R.; Varela, M.; Borisevich, A. Y.; Peng, Y.; Oxley, M. P.; Chisholm, M. F. In Scanning Microscopy for Nanotechnology: Techniques and Applications; Zhou, W., Wang, Z. L., Eds.; Springer, Netherlands, **2006; pp 152–191.**
24. Kucukayan, G.; Ovali, R.; Ilday, S.; Baykal, B.; Yurdakul, H.; Turan, S.; et al. *Carbon* **2011,** *49*, 508.